Pflugers Arch - Eur J Physiol (2008) 456:1121–1136
DOI 10.1007/s00424-008-0468-7

VAMP2 interacts directly with the N terminus of Kv2.1 to enhance channel inactivation

Anatoli Lvov · Dodo Chikvashvili · Izhak Michaelevski · Ilana Lotan

Received: 19 November 2007 / Revised: 6 January 2008 / Accepted: 22 January 2008 / Published online: 10 June 2008

Abstract Recently, we demonstrated that the Kv2.1 channel plays a role in regulated exocytosis of dense-core vesicles (DCVs) through direct interaction of its C terminus with syntaxin 1A, a plasma membrane soluble NSF attachment receptor (SNARE) component. We report here that Kv2.1 interacts with VAMP2, the vesicular SNARE partner that is also present at high concentration in neuronal plasma membrane. This is the first report of VAMP2 interaction with an ion channel. The interaction was demonstrated in brain membranes and characterized using electrophysiological and biochemical analyses in *Xenopus* oocytes combined with an in vitro binding analysis and protein modeling. Comparative study performed with wild-type and mutant Kv2.1, wild-type Kv1.5, and chimeric Kv1.5N/Kv2.1 channels revealed that VAMP2 enhanced the inactivation of Kv2.1, but not of Kv1.5, via direct interaction with the T1 domain of the N terminus of Kv2.1. Given the proposed role for surface VAMP2 in the regulation of the vesicle cycle and the important role for the sustained Kv2.1 current in the regulation of dendritic calcium entry during high-frequency stimulation, the interaction of VAMP2 with Kv2.1 N terminus may contribute, alongside with the interaction of syntaxin with Kv2.1 C terminus, to the activity dependence of DCV release.

Keywords Kv2.1 · VAMP2 · Inactivation · T1 domain

Introduction

The *Shab* subfamily of the voltage-gated K^+ (Kv) channels, including Kv2.1 and Kv2.2 members [20, 24], are major molecular determinants of a slow-inactivating delayed rectifier current in neuronal [45], neuroendocrine, and endocrine cells [41, 51]. Specifically, Kv2.1 channels are located mainly on the soma and dendrites of hippocampal neurons [14, 23], and their sustained current regulates spike duration and, consequently, dendritic calcium entry during high-frequency stimulation, suggesting a role for Kv2.1 in the fidelity of high-frequency synaptic transmission [13]. To date, there is a constantly growing list of experimental data indicating interaction of syntaxin 1A (Syx) and SNAP-25, the two plasma-membrane-associated protein components of the soluble NSF attachment receptor (SNARE) complex (t-SNAREs) that is essential to the exocytotic process [5], with various voltage-gated calcium (for review, see [15]) and potassium channels. Regarding Kv channels, it was previously shown that Kv1.1 interacts with Syx in brain synaptosomes and in oocytes [17], and Kv2.1 and Kv2.2 interact with Syx and SNAP-25 in PC12 cells, islet β-cells, and *Xenopus* oocytes [26, 36, 41, 44, 58, 62]. The physical interactions of Kv2.1 with Syx and the t-SNARE complex have distinct effects on Kv2.1 gating [44, 58], whereas Kv2.2 gating is affected only by Syx [62].

Electronic supplementary material The online version of this article (doi:10.1007/s00424-008-0468-7) contains supplementary material, which is available to authorized users.

Anatoli Lvov and Dodo Chikvashvili are equal contributors.

A. Lvov · D. Chikvashvili · I. Lotan (✉)
Department of Physiology and Pharmacology,
Sackler Faculty of Medicine, Tel-Aviv University,
69978 Ramat-Aviv, Israel
e-mail: ilotan@post.tau.ac.il

I. Michaelevski
Department of Biological Chemistry,
Weizmann Institute of Science,
76100 Rehovot, Israel

VAMP2 (synaptobrevin), the neuronal-vesicle-associated partner (v-SNARE) of the SNARE complex [8, 52] plays essential role in synaptic vesicles exocytosis [53] and is also important in secretion from endocrine cells (e.g., pancreatic β-cells; [6]). Similarly to the t-SNAREs that network with various proteins, VAMP2 participates in different protein–protein interactions [19, 47, 48]. In contrast to the t-SNAREs, to date, no evidence has been presented concerning interaction of VAMP2 with ion channels. However, taking into account its participation in protein–protein interactions together with its now well-established presence at high concentration on axonal surface [16, 56], forming a steady-state reservoir [12], it is not inconceivable that VAMP2 may interact either directly or indirectly, through its protein partners, with ion channels. In this study, we report physical and functional interactions of plasma membrane VAMP2 with Kv2.1 and Kv2.2, affecting mainly the steady-state and kinetic properties of their inactivation. These results suggest a role for the Kv2.1–VAMP2 interaction in dense-core vesicles (DCVs) release of hormones, neuropeptides, or neurotrophins from dendrites and endocrine cells where the channels are localized.

Notably, Kv2 channels undergo slow U-shaped inactivation from preferentially closed state [30, 31], which differs in several parameters from classical C-type inactivation, characterized in *Shaker* channels (reviewed in [34]). To date, structure–function studies have provided little insight into the structural basis for Kv2.1 'U-type' inactivation, although several structural manipulations within the N-terminal tetramerization T1 domain and association with modulatory α-subunits implicate both the N terminus and the S6 segment in this inactivation [28, 29] (for review, see [34]). Using various Kv2.1 truncated channels and a Kv1.5-Kv2.1 chimeric channel, we show in this study that in contrast to the interaction with either Syx or the t-SNARE complex, the interaction with VAMP2 does not involve the C terminus of Kv2.1. Rather, it requires the N terminus of the channel, specifically an extension of a docking loop within the T1 domain that is absent in Kv1.5. These results extend our knowledge of the structural determinants that confer K^+ channel inactivation.

Materials and methods

Constructs and antibodies The antibodies used were: polyclonal antibodies against Kv2.1 C terminus or Kv2.1 N terminus (Alomone Labs, Jerusalem, Israel) and polyclonal antibody against VAMP2 (Abcam, Cambridge, UK). Kv2.1 wild-type and its C-terminal (ΔC318 and ΔC416) and N-terminal (ΔN119) truncation mutants (kindly provided by Prof. R. Joho, The University of Texas Southwestern Medical Center, Dallas, TX, USA) complementary DNAs (cDNAs) were cloned in pBluescript. Kv1.5 (kindly provided by Prof. B. Attali, Tel-Aviv University, Israel) Kv1.5N/Kv2.1 (kindly provided by Prof. David Fedida, University of British Columbia, Vancouver, Canada), Kv2.1ΔN139, and BoNT/C (kindly provided by Dr. H. Gaisano, University of Toronto, Ontario, Canada) cDNAs were cloned in pCDNA3. To generate $Kv2.1\Delta N_{70–73}$ (deletion of four amino acids), oligonucleotide primers: 5′ CGACTCCCTGCTCCAGGTGTGCCTTGAGGACAAC GAGTACTTC and 5′ GAAGTACTCGTTGTCCT CAAGGCACACCTGGAGCAGGGAGTCG were used to amplify wild-type Kv2.1 by QuikChange® site-directed mutagenesis kit (Stratagene, La Jolla, CA, USA), according to the manufacturer's instruction manual. Kv2.2 (kindly provided by Prof. O. Pongs, Zentrum fur Molecular Neurobiologie, University of Hamburg, Germany) cDNA was cloned in pGEMHE. Kv2.1/Kv2.3T1-S1 (Kv2.1/Kv2.3NRD) cDNA (kindly provided by Prof. José López-Barneo, Universidad de Sevilla, Seville, Spain) was cloned in p513 eukaryotic expression vector (derivative of pSG5, Stratagene). Preparation of messenger RNAs (mRNAs) was as described [37]. The degenerate phosphorothioate antisense oligodeoxynucleotides targeted against syntaxins (AS-Syx) was created as described [43]. DNAs of Kv2.1 fragments for generation of GST fusion proteins were constructed as described [44]. His-6-tagged VAMP-2 (kindly provided by Dr. Michael Veit, Free University, Berlin, Germany) was cloned to pQE30 and purified as described [27].

Electrophysiological recording in oocytes Preparation of *Xenopus laevis* oocytes was performed as described [37]. Typically, for the electrophysiological assays, oocytes were injected with the following concentrations of mRNA (further detailed in the figure legends): 0.025–0.1 ng/oocyte of Kv2.1 and its C-terminal deletion mutants; 0.05 ng/oocyte of Kv1.5; 2.5 ng/oocyte of $Kv2.1\Delta N_{70–73}$ and Kv2.1N/Kv1.5; 0.008–0.14 ng/oocytes of Kv2.2; 1.5 ng/oocyte of VAMP2 and 5–15 ng/oocyte of BoNT/C. Fifty nanograms per oocyte AS-Syx was injected 2 days before the electrophysiological assay, which was performed 3 days after the mRNA injection. Two-electrode voltage-clamp recordings were performed as described [38]. To avoid possible errors introduced by series resistance, only current amplitudes up to 6 μA were recorded. Net current was obtained by subtracting the scaled leak current elicited by a voltage step from −80 to −90 mV. Oocytes with a leak current of more than 3 nA/1 mV were discarded. Experimental protocols and data analyses are described in the figure legends.

Immunoprecipitation in oocytes For the biochemical assays, oocytes were injected with 5–15 ng/oocyte of

Kv1.5, Kv2.1, Kv2.2 and all mutants, and with 0.25–1.5 ng/oocyte of VAMP2 (further detailed in the Figure legends). Oocytes were subjected to immunoprecipitation (IP) as described [38]. Briefly, immunoprecipitates from 1% Triton X-100 lysates of either plasma membranes (PMs) or internal fractions (IFs) (separated mechanically, as described [25]) were analyzed by sodium dodecylsulfate–polyacrylamide gel electrophoresis (SDS-PAGE; both 8% and 12% of acrylamide). Digitized scans were derived by PhosphorImager (Molecular Dynamics, Eugene, OR, USA) and relative intensities were quantitated by ImageQuant.

In vitro binding of GST fusion proteins with His-6-tagged VAMP2 The fusion proteins were synthesized and reacted with VAMP2 as described [17]. Briefly, purified GST fusion proteins (100–200 pmol) immobilized on glutathione-Sepharose beads were incubated with 200 pmol (or different concentrations as denoted in Fig. 6b) of His-6-tagged VAMP2 in 1ml phosphate-buffered saline (PBS) containing 0.1% Triton X-100. After washing, the GST fusion proteins were eluted with 20 mM reduced glutathione in 40 μl of elution buffer (120 mM NaCl, 100 mM Tris–HCl, pH8), separated by 12% SDS-PAGE, and subjected to Western blot analysis using the ECL Detection System (Pierce, Rockford, IL, USA); proteins in nitrocellulose membrane were stained by Ponceau.

Immunoprecipitation and immunoblotting in rat brain membranes Crude rat brain membranes (P2 fraction) were prepared as described [39], stored in aliquots of 150–200 mg at −80°C, and thawed once right before using. Aliquots were solubilized in PBS buffer containing 2% CHAPS and a mixture of protease inhibitors (Boehringer, Mannheim) and subjected to IP and immunoblotting (IB), essentially as described previously [17].

"Pull-down" from rat brain membranes GST fusion proteins (200 pmol) were incubated with 150–200 mg crude rat brain membranes (P2 fraction) in PBS buffer with 2% CHAPS and a mixture of protease inhibitors (Boehringer) at 4°C overnight and then immobilized on glutathione-Sepharose beads. Samples were washed four times with PBS containing 0.1% CHAPS then boiled for 10min in SDS sample buffer. IB and visualization were performed as described above.

Protein modeling Three-dimensional models for the T1 domains of Kv1.5 and Kv2.1 channels were created using 3Djigsaw prediction algorithm for comparative modeling [3]. Kv1.2 (PDB 2a79, chain B) was chosen as a structural template because in pairwise comparison with both Kv2.1 and Kv1.5, it received the highest 100 bit score among different candidates: 5.38521 with Kv1.5 and 4.85556 with Kv2.1 (according to authors' empirical data, if the bit score is above 2, then 95% of alignments are accurate). The obtained models were superimposed in Swiss-PDBViewer 3.7 with Magic Fit (http://www.expasy.org/spdbv/).

Statistical analysis Data are presented as means ± SE. The statistical significance of differences between the two groups was calculated by the use of independent sample *t* test procedures assuming unequal variance (Mann–Whitney's rank-sum test). Multiple group comparisons were done using one-way analysis of variance (ANOVA) followed by Holm–Sidak test for multiple comparisons. All the statistical analyses were performed using SigmaStat 3.1 for Windows (Systat Software, USA).

Results

VAMP2 affects steady-state and kinetic parameters of Kv2.1 inactivation In an effort to analyze functional and physical interactions between VAMP2 and Kv2.1, we employed the heterologous expression system of *Xenopus* oocytes in which biochemical and electrophysiological analyses were carried out concomitantly. Co-injection of Kv2.1 with high concentration (≥1.5 ng/oocyte) of VAMP2 mRNAs into oocytes occasionally decreased the outward K^+ current amplitudes and affected the Kv2.1 activation and inactivation gating, assayed by two-electrode voltage-clamp technique. Biochemical analysis demonstrated that the reduced currents correlated with impaired trafficking of the channels to the plasma membrane (unpublished results). Accumulated experimental data demonstrated that the effect on Kv2.1 activation gating was inconsistent—it was evident in only a few batches of oocytes. In contrast, the effect on inactivation was reproducible: It appeared in all batches of oocytes and was already apparent with lower VAMP2 mRNA concentrations that did not affect the current amplitudes, arguing that the effects on current amplitude and on inactivation gating were independent. Further, to exclude any possible link between the two effects that may lead to experimental artifacts, the effect of co-expressed VAMP2 on gating was always assayed in oocytes expressing current amplitudes comparable to those expressed in its absence.

The effect of VAMP2 on Kv2.1 voltage dependence of steady-state inactivation (SSI) was studied using depolarizing prepulses followed by a test pulse to +50 mV (Fig. 1a, upper panel). The main characteristic of Kv2.1 inactivation is U-shaped voltage dependence (see Fig. 1d), with initial decline of inactivation curve up to about 0 mV followed by an "upturn" in the voltage dependence at strong depolarization [31]. In our analysis, we referred only to the declining

phase of the inactivation curve and fitted it with a one-component Boltzmann equation (Fig. 1b). As Kv2.1 currents inactivate slowly upon membrane depolarization (Fig. 1a), we started with 30-s prepulses (Fig. 1b), which induce maximal inactivation. Co-injection of VAMP2 with Kv2.1 mRNAs resulted in a negative shift of the half-inactivation voltage ($Vi_{1/2}$) by about 10 mV (Fig. 1b, inset), with no effect on the slope factor (not shown). For practical reasons, all subsequent studies of Kv2.1 SSI were done with 5-s prepulses, which yielded quite similar shifts in $Vi_{1/2}$; however, an increase in the non-inactivating current fraction became apparent with the short prepulses in oocytes expressing VAMP2 (Fig. 1c,d), probably due to the effect of VAMP2 to enhance the rate of inactivation (see below). These shifts in $Vi_{1/2}$ showed clear dependence on the amount of injected VAMP2 mRNA (Fig. 1e,f).

Analysis of the effect of VAMP2 on the kinetic parameters of Kv2.1 current revealed that whereas VAMP2 did not change the activation time constant, it accelerated the onset of inactivation [Electronic supplementary material (ESM), Fig. S1] and decreased the rate of recovery from inactivation (ESM, Fig. S2) at voltages near or below of Kv2.1 $Va_{1/2}$ [44] that favor occupancy of partially activated closed states. In all, rendering the SSI more sensitive to depolarization, speeding up the onset of inactivation, and attenuating the recovery from inactivation, VAMP2 promotes the inactivation state of Kv2.1.

As the effects of VAMP2 on Kv2.1 inactivation were similar to those previously demonstrated for Syx [44], we looked into the possibility that VAMP2 exerts its effects indirectly via interaction with the oocyte's endogenous Syx. To this end, we assayed the effects of VAMP2 in oocytes of which endogenous Syx was knocked down [44, 58] by injecting an antisense oligodeoxinucleotide, which is directed against highly conserved stretches of the linker domain separating the H2B and H3 helixes of Syx (AS-Syx; blocks de novo synthesis of Syx) together with mRNA encoding the light chain of Botulinum neurotoxin C (BoNT/C; selectively cleaves already synthesized Syx). Figure 1f demonstrates that the effect of VAMP2 is not mediated by endogenous Syx.

VAMP2 affects both steady-state and kinetic parameters of Kv2.2 inactivation similarly to Kv2.1 Previously, we showed that due to major sequence divergence of the C terminus of Kv2.2 from that of Kv2.1 [mainly distal to the C1a region (see Fig. 2a) where Kv2.1 and Kv2.2 exhibit only 24% sequence identity], the interactions of Kv2.2 with Syx and with the t-SNARE complex were different from those of Kv2.1 [62]. Here, we tested the interaction of Kv2.2 with VAMP2. Co-expression of VAMP2 caused a significant leftward shift of $Vi_{1/2}$ (Fig. 2d,e). In addition, inactivation onset was accelerated at voltages near or below

Fig. 1 VAMP2 affects the voltage dependence of Kv2.1 steady-state inactivation. **a** Representative current traces demonstrating Kv2.1 steady-state inactivation (*SSI*, leak subtracted) from a single oocyte injected with Kv2.1 only (*Kv2.1*) or with 1.5 ng/oocyte VAMP2 (*+VAMP*) mRNAs. Currents were elicited by 30-s depolarizing prepulses applied from −80 mV in ascending order (V_{prepulse}) followed by a 350-ms test pulse to +50 mV (*upper panel*). A representative experiment demonstrating the effects of VAMP2 on Kv2.1 SSI, performed in a single batch of oocytes (five oocytes per group) using the 30-s inactivation protocol, is shown in **b**; normalized current amplitudes ($I/I_{\max}$) were plotted as function of V_{prepulse}. Data from each oocyte were fitted to the Boltzmann charge-voltage sigmoidal equation $\left(I/I_{\max} = 1\Big/\left(1+\exp^{-\left(V_{prepulse}-Vi_{1/2}\right)/a}\right)+C\right)$, and mean values of half inactivation ($Vi_{1/2}$) drawn from three independent experiments are shown in the *inset*. **c** representative Kv2.1 current traces obtained by application of a 5-s inactivation protocol (*upper panel*; same as in **a** and **b**, but with 5-s depolarizing prepulses) from a single oocyte injected with Kv2.1 only (*Kv2.1*) or with 1.5 ng/oocyte VAMP2 *(+VAMP)* mRNAs. **d** A representative experiment, performed with the 5-s inactivation protocol, demonstrating the full U-shaped inactivation curves of Kv2.1. **e** A representative experiment demonstrating the dependence of Kv2.1 $Vi_{1/2}$ on the VAMP2 mRNA concentration (two different concentrations, as denoted). **f** Summarized $Vi_{1/2}$ values obtained from several experiments as in **e**. Statistical differences between groups were estimated by the one-way ANOVA analysis, as described in "Materials and methods"; $^{**}P=<0.001$ [for the differences in the mean $Vi_{1/2}$ values among the treatment groups, as estimated by one-way ANOVA; in pairwise multiple comparison procedures (Holm–Sidak method), the overall significance level= 0.05]. **g** Knockdown of the endogenous Syx by injection of a mixture of AS-Syx and Botulinum neurotoxin C mRNA *(+AS-Syx + BoNT/C)* did not impair the effect of VAMP2 on the voltage dependence of Kv2.1 inactivation. Oocytes injected with Kv2.1 only or together with VAMP2 mRNAs were either co-injected or not with the mixture. Five oocytes per group were assayed. In all *bar diagrams*, *numbers within* and *without parentheses* denote the number of batches and the total number of oocytes per group, correspondingly; the same batches were tested for the all groups

$Va_{1/2}$ (ESM, Fig. S3). Thus, Kv2.1 and Kv2.2 exhibited similar functional interactions with VAMP2.

VAMP2 associates with Kv2.1 and Kv2.2 Concomitantly with the functional experiments, we examined the physical interactions of VAMP2 with Kv2.1 and Kv2.2 proteins in oocytes. SDS-PAGE analysis of metabolically labeled proteins in both the IF (consisting of cytoplasm and intracellular organelles; Fig. 3a) and PM (manually dissected; Fig. 3b) of oocytes, using antibody raised against the very end of their N termini (*IP Kv*), showed that VAMP2 co-immunoprecipitated both with Kv2.1 and Kv2.2. Significant associations were detected in a variety of detergents including 1% CHAPS and in 1% Triton X-100. The specificity of the interactions was further verified by reciprocal co-immunoprecipitation of the channels with VAMP2 using anti-VAMP2 antibody (*IP VAMP*).

Kv2.1 C terminus is not necessary for the effect of VAMP2 on Kv2.1 inactivation The conservation of the VAMP2 interaction, both functional and physical, in Kv2.2 suggested

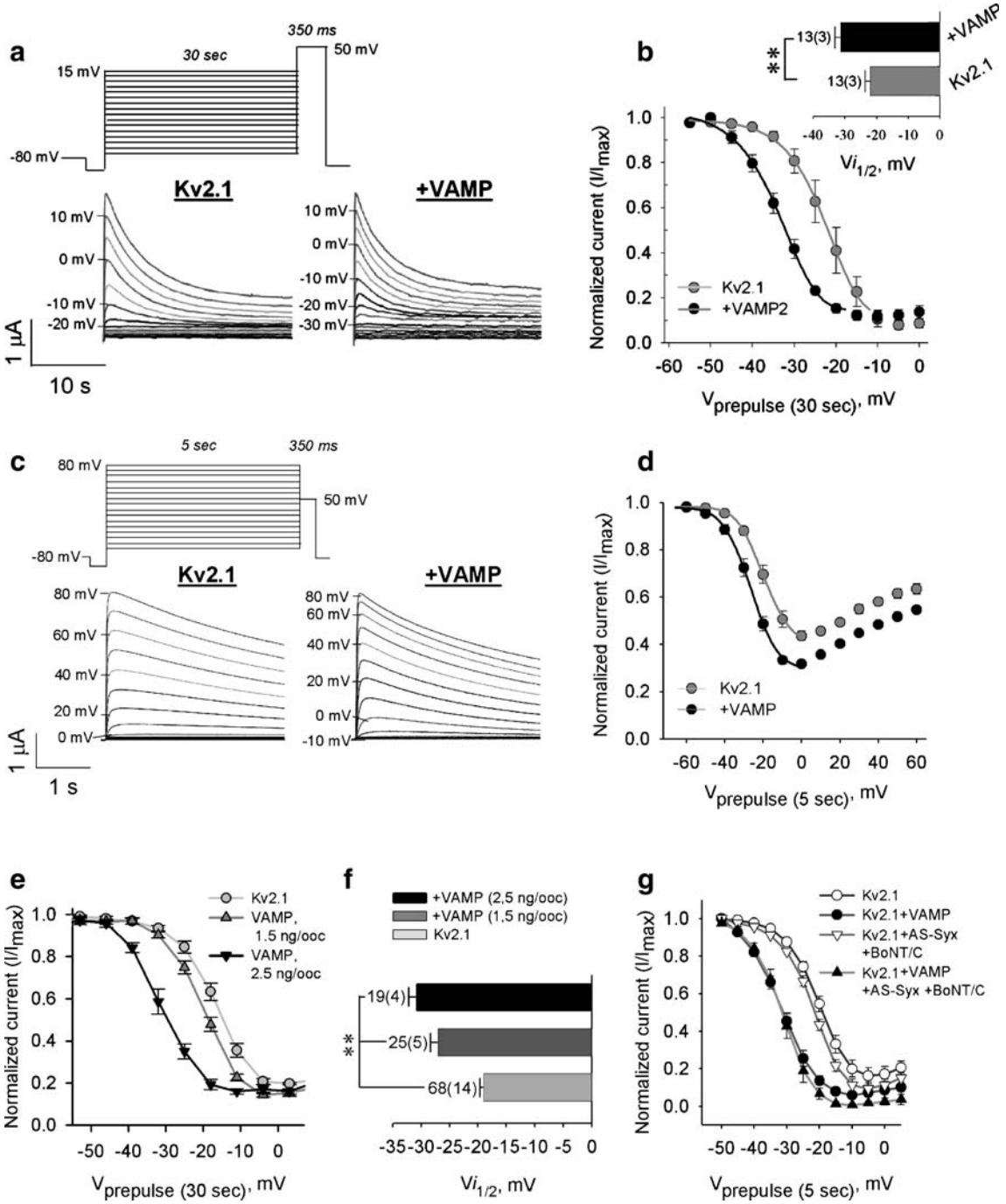

that the C-terminal portion distal to C1a did not participate in this interaction. We aimed to further probe the involvement of the whole Kv2.1 C terminus in the interaction using the C-terminal deletion mutants Kv2.1ΔC416 and Kv2.1ΔC318 (missing the last 416 and 318 amino acids, respectively; Fig. 4a) [59]. We compared the effects of VAMP2 on the SSI of these mutants versus wild-type channels that were expressed in the same batch of oocytes and assayed on the same day. The VAMP2 effect was conserved in both ΔC416 and ΔC318 (Fig. 4b–d), in contrast to the effects of both Syx and the t-SNARE complex that were previously shown to dissipate [58], indicating that Kv2.1 C terminus does not mediate the VAMP2 effect. In parallel, we examined the direct association of VAMP2 with ΔC416 and ΔC318 in co-immunoprecipitation experiments (Fig. 4e) and calculated the ratio of the amount of co-precipitated VAMP2 to the amount of precipitated mutant protein and normalized it to that of Kv2.1 ("normalized binding"; Fig. 4e, inset). The two C-terminal truncations, which did not affect the functional interaction with

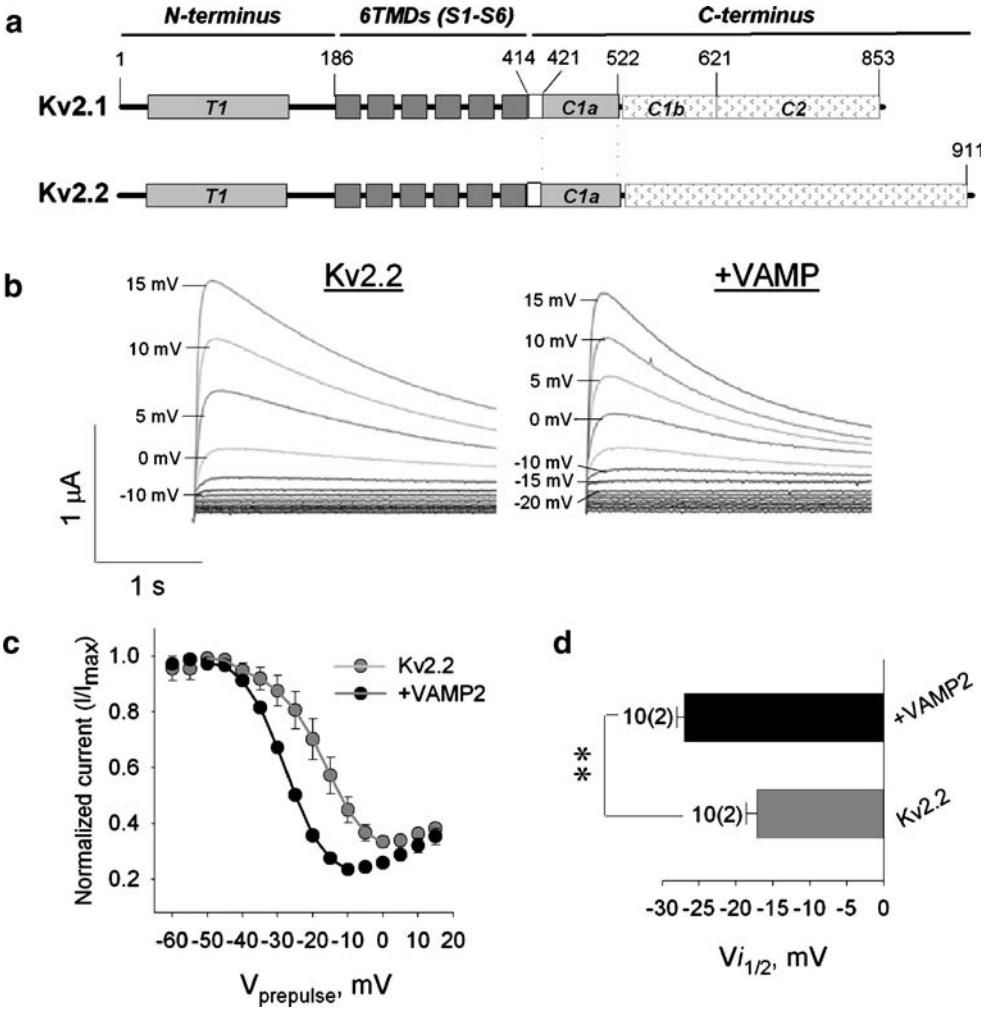

Fig. 2 Effects of VAMP2 on Kv2.2 are similar to those of Kv2.1. **a** Schematic presentation of Kv2.1 and Kv2.2 channels; *numbers* denote amino acids. **b** Representative Kv2.2 current traces obtained from single oocyte, injected with Kv2.2 only (*Kv2.2*) or with VAMP2 (*+VAMP*) mRNAs and subjected to the 5-s inactivation protocol. **c**, **d**, Effect of VAMP2 on the voltage dependence of Kv2.2 inactivation. A representative experiment with five oocytes per group injected with Kv2.2 only or with VAMP2 mRNAs is shown in **c**. The mean $Vi_{1/2}$ values, derived as described in the legend for the Fig. 1b, are compared in **d**

VAMP2, exhibited a substantial reduction of VAMP2 binding (by 55% and 65%).

Kv2.1 N terminus is essential for the effect of VAMP2 on Kv2.1 inactivation The N terminal T1 domain of K^+ channels has been implicated in several important functions, including inter-subunit interactions during channel assembly, binding to other domains of the full-length channel or to other proteins and participation in channel gating (see "Discussion"). Recently, it was demonstrated that the Kv2.1 T1 domain is a regulatory site for the U-type inactivation [35], suggesting it as a potential candidate that is involved in the effect of VAMP2 on Kv2.1 inactivation. However, before examining the involvement of T1, we excluded the possible involvement of the linker which connects T1 to the first transmembrane segment (S1). The T1–S1 linker (amino acids 148–186; termed NRD [10]) was implicated in Kv2.1 gating and interaction with the auxiliary subunit Kv2.3 (or Kv8.1). Thus, we tested the effect of VAMP2 on Kv2.1/Kv2.3T1-S1 (Fig. 5a), a chimeric Kv2.1 channel in which the T1–S1 linker was replaced by the corresponding Kv2.3 sequence (these two sequences share < 20% identity). As expected, the replacement of the T1–S1 linker did not affect significantly the response of the channel to VAMP2 (Fig. 5b,c) and did not impair the association of the channel with VAMP2 (Fig. 5g).

To study the involvement of the T1 domain in the VAMP2 effect, we could not use T1 deletion mutants (ΔN119 or ΔN139; lacking the first 119 or 139 amino acids, correspondently; see Fig. 5a), which did not express K^+ currents (both truncations are within the T1 domain that is important for channel assembly and gating). To circumvent this problem, we took advantage of our finding that Kv1.5 does not interact functionally or physically with VAMP2 (Fig. 5d and g, respectively). Thus, we used a chimeric channel, Kv1.5N/Kv2.1, in which the whole N terminus of Kv2.1 was replaced with that of Kv1.5 (see Fig. 5a; [35]). Kv1.5N/Kv2.1 interacted neither functionally (Fig. 5e,f) nor physically (Fig. 5g) with VAMP2. These results indicated that Kv2.1 N terminus, which by itself modulates Kv2.1 U-shaped inactivation [33, 35], also mediates the modulation of this inactivation by VAMP2.

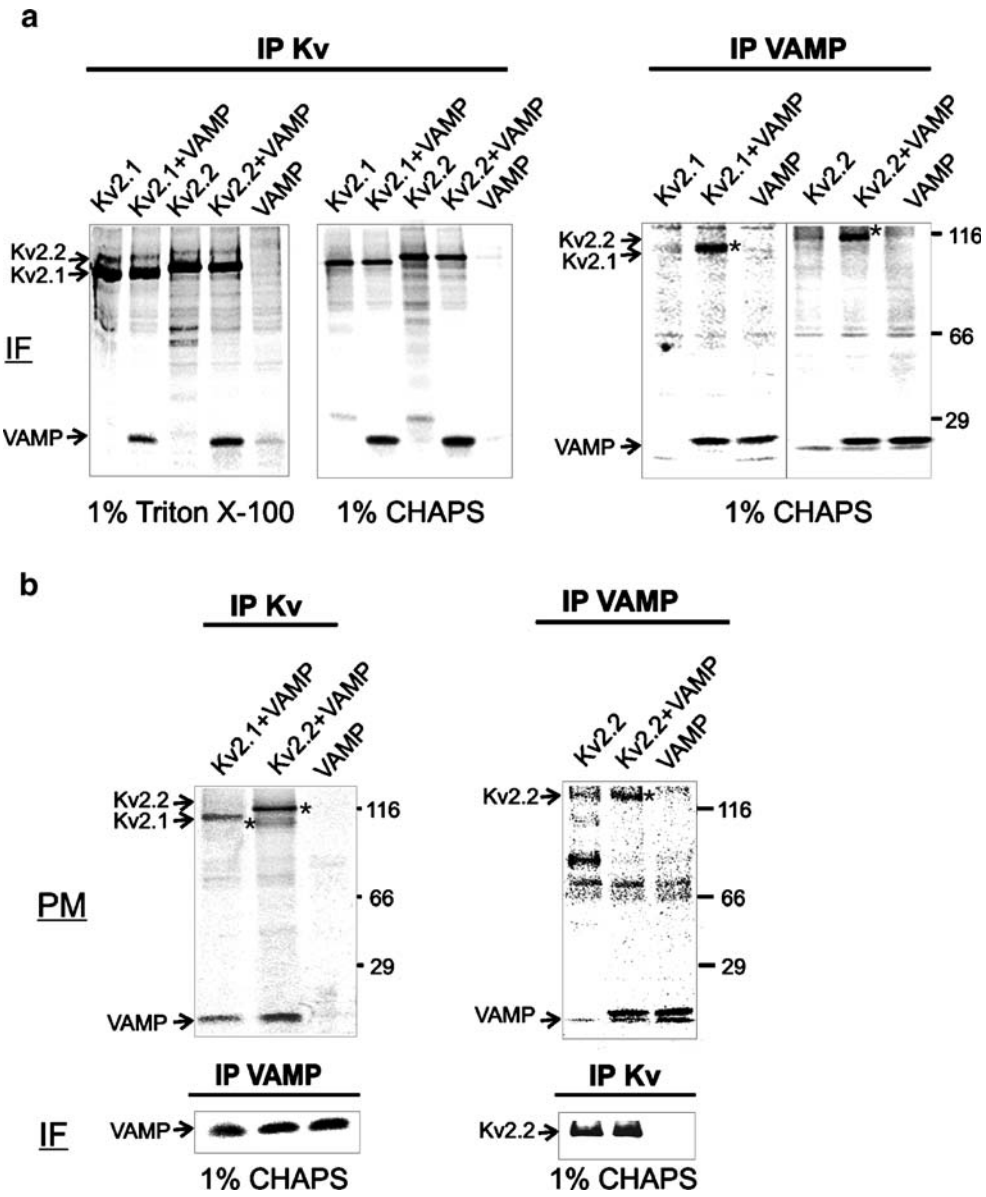

Fig. 3 Kv2.1 and Kv2.2 channels interact physically with VAMP2 in *Xenopus* oocytes. **a**, **b** Digitized PhosphorImager scans of SDS-PAGE analysis of reciprocal co-immunoprecipitation of [^{35}S]Met/Cys-labeled Kv2.1, Kv.2.2 and VAMP2 proteins from 1% CHAPS lysates of internal fractions (*IF*) (**a**) or plasma membranes (*PM*) (**b**) of oocytes. Relevant proteins were co-immunoprecipitated by Kv2.1 (*IP Kv*) or VAMP2 (*IP VAMP*) antibodies. Oocytes (from a single batch) were injected with Kv2.1 or Kv2.2 only (*Kv2.1; Kv2.2*), co-injected with VAMP2 (*+VAMP*), or injected with VAMP2 only (*VAMP*), as indicated *above the lanes*. An additional experiment performed with 1% Triton X-100 lysates is presented in **a**. To demonstrate that the total amount of proteins was similar in all relevant groups of oocytes used in the reciprocal analysis of PM (**b**, *upper panels*), the complement analysis of IF is also presented (*lower panels*). *Numbers on the right* refer to the mobility of pre-stained molecular mass standards. *Arrows on the left* indicate the migration of the denoted proteins (also marked with *asterisks* on the gel scans)

A clear correlation between the functional and physical interactions with VAMP2 emerged from the analyses of the C-terminal (Fig. 4) and N-terminal (Fig. 5) mutant channels: Those that responded to VAMP2 also bound it (albeit the binding was reduced in the case of the C-terminal truncated channels, possibly due to conformational changes induced by the major truncations), whereas the one that did not bind VAMP2 was unaffected by VAMP2. This correlation prompted us to investigate the possible existence of a causative relationship between the physical and the functional interactions of VAMP2 with Kv2.1 (see in the following).

Physical interaction between Kv2.1 and VAMP2 in plasma membranes mediates the effect on inactivation: a critical role for the N terminus The failure of VAMP2 to interact with Kv1.5N/Kv2.1 implicated the participation of the N terminus in VAMP2 binding. To further substantiate this notion, we performed an in vitro binding assay using immobilized GST fusion protein corresponding to the whole N terminus (GST-$N_{1\text{-}184}$) with recombinant His6-tagged VAMP2 (Fig. 6a). The results of both settings were similar and demonstrated a direct in vitro binding between VAMP2 and Kv2.1 N terminus. Further, using different concentrations of VAMP2, we estimated that under our binding conditions, the binding was half-maximal at 0.07–0.08 μM of VAMP2 and that about 10 pmol of VAMP2 were bound per 20 pmol of GST-N at a saturating VAMP2 concentration (Fig. 6b).

Next, taking advantage of the fact that the GST-$N_{1\text{-}184}$ peptide bound well VAMP2 and could probably compete well with the binding of VAMP2 to the channel expressed

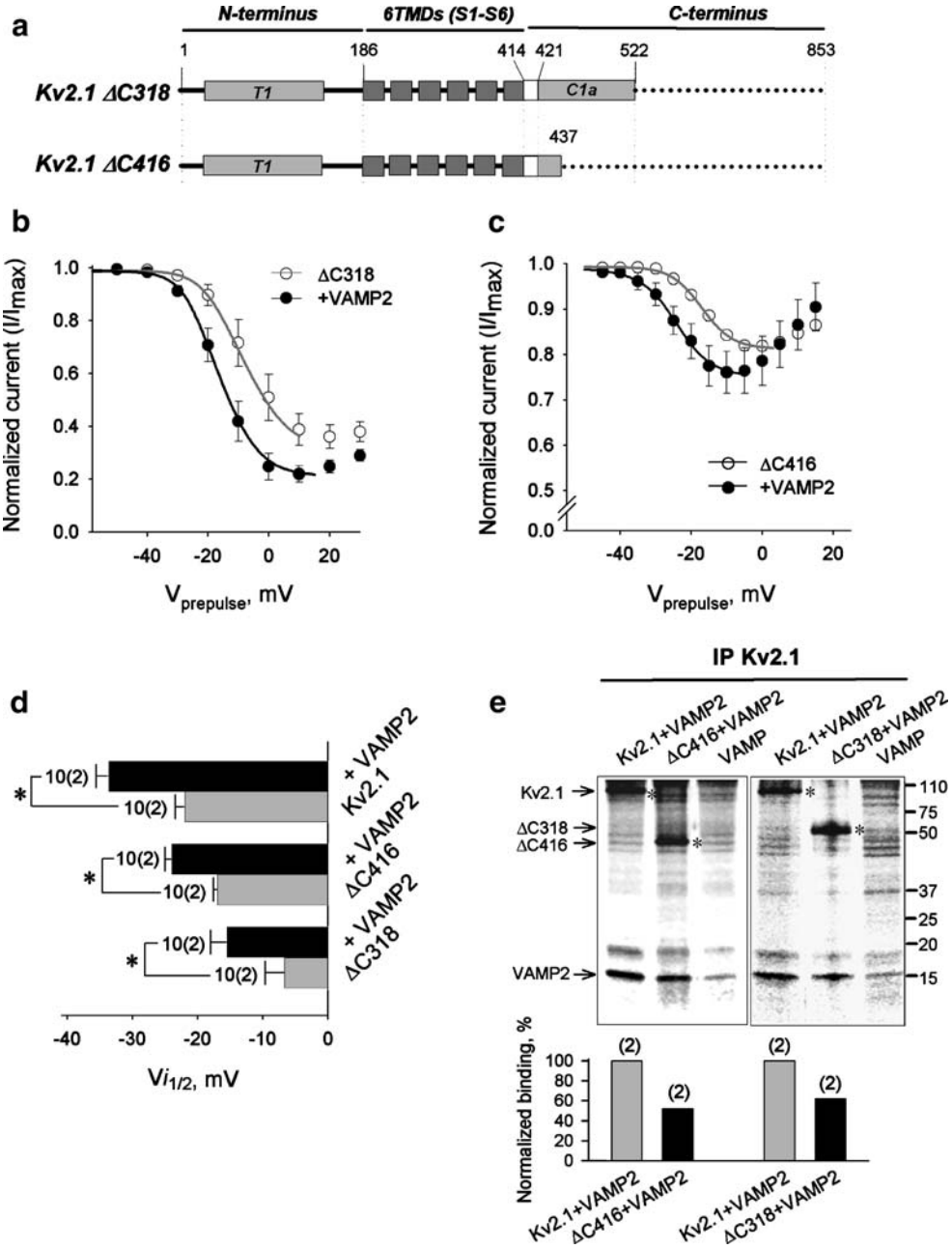

Fig. 4 Partial deletions of the Kv2.1 C terminus do not abolish the effect of VAMP2 on inactivation and reduce, but do not eliminate the association of VAMP2 with Kv2.1. **a** Schematic presentation of two Kv2.1 C-terminal deletion mutants; *numbers* denote amino acids. **b**–**d** Effects of VAMP2 on ΔC318 (**b**) and ΔC416 (**c**) inactivation. Representative experiments with five oocytes per group derived as in Fig. 2b are shown. *Bar diagrams* in **d** show the mean ΔC318 and ΔC416 $Vi_{1/2}$ values derived from two independent experiments and compared with the wild-type Kv2.1 $Vi_{1/2}$ values from the same batches of oocytes; $*p<0.05$. **e** Digitized Phosphorimager scan of SDS-PAGE analysis of co-immunoprecipitation of [^{35}S] Met/Cys-labeled Kv2.1, ΔC318, ΔC416, and VAMP2 proteins from 1% CHAPS lysates of whole oocytes of a single batch. The proteins were immunoprecipitated by an antibody raised against the N terminus of Kv2.1 (*IP Kv2.1*). Oocytes were injected with the channels together with VAMP2 mRNAs or injected with VAMP2 mRNA only (as denoted above the *lanes*). The *bar diagram* below the scan presents relative intensity quantification of co-precipitated VAMP2 normalized to the precipitated channel. Molecular weight markers are shown on the *right*. *Arrows on the left* indicate the migration of the denoted proteins (also marked with *asterisks*). The results shown are from two independent experiments

in oocytes, we investigated the possible existence of a causative relationship between the binding of VAMP2 to Kv2.1 and its effect to enhance inactivation. Thus, we tried to acutely rescue the channel from the functional effects of VAMP2 by microinjection of the GST-$N_{1\text{-}184}$ peptide into oocytes already expressing Kv2.1 with VAMP in the plasma membrane. As a control, we used GST, which did not bind VAMP2. As shown in Fig. 7, the leftward shift in the steady-state inactivation curve caused by co-expressed VAMP2 could indeed be reversed by GST-$N_{1\text{-}184}$. GST itself had no effect, confirming that GST-$N_{1\text{-}184}$ attenuates the effect of VAMP2 by disrupting its interaction with Kv2.1. The results of this experiment point to a link between the effect of VAMP2 on inactivation and its physical interaction with the functional channel in the plasma membrane. Moreover, they further highlight the binding at the N terminus as critical for the VAMP2 interaction.

An extension of a docking loop at the lateral part of T1 could be important for the interaction with VAMP2 The above results suggested that the T1 domain of Kv2.1, but not of Kv1.5, mediates VAMP2 binding and effect on inactivation. To explore the differences between the T1 domains of Kv2.1 and Kv1.5 that may be responsible for their different interactions with Kv2.1, we created 3D models for the T1 domains of both channels (Fig. 8a). The

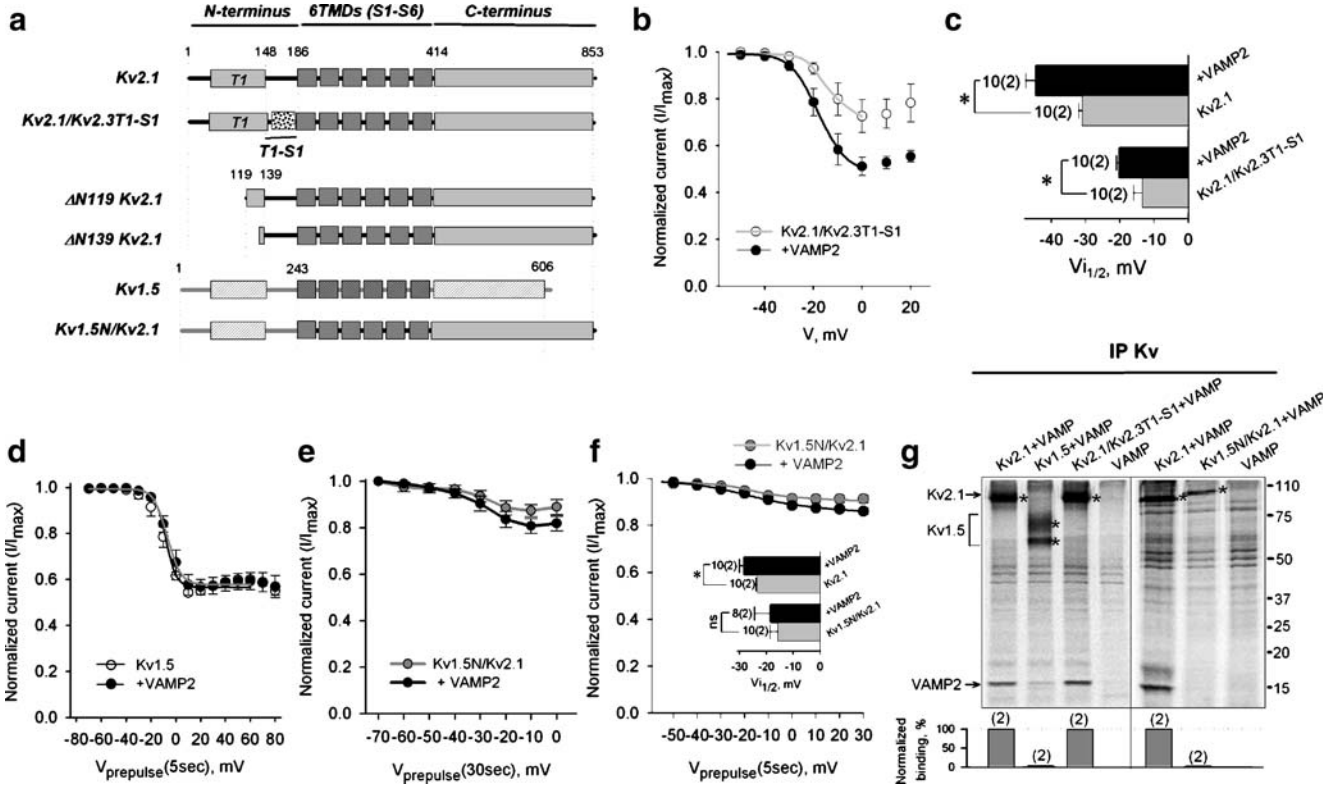

Fig. 5 Interactions of different Kv2.1 N-terminal chimeric channels with VAMP2. **a** Schematic presentation of N-terminal chimeric channels; *numbers* denote amino acids. **b**, **c** VAMP2 affects Kv2.1/Kv2.3T1-S1 inactivation. A representative experiment with 5-s inactivation protocol (**b**) and mean $Vi_{1/2}$ values (**c**) compared with those of *WT* Kv2.1 in the same batches of oocytes, derived from two independent experiments;*$p<0.05$. **d** VAMP2 did not affect inactivation of wild-type Kv1.5 in a representative experiment. **e**, **f** VAMP2 did not affect the inactivation of Kv1.5N/Kv2.1. A representative experiment with 30-s (**e**) and 5-s (**f**) inactivation protocols and mean $Vi_{1/2}$ values (**f**, *inset*) compared with those of *WT* Kv2.1 in the same batches of oocytes, derived from two independent experiments; *$p<0.05$. **g** Digitized Phosphorimager scan of SDS-PAGE analysis of [^{35}S]Met/Cys-labeled Kv2.1/Kv2.3T1-S1, Kv1.5, and Kv1.5N/Kv2.1 channels injected with VAMP2 and immunoprecipitated by an antibody raised against the N terminus of Kv2.1 or Kv1.5, correspondingly (*IP Kv*). The *bar diagram* below the scan demonstrate relative intensity quantification of co-precipitated VAMP2 normalized to the precipitated channel. Molecular weight markers are shown on the *right*. *Arrows on the left* indicate the migration of the denoted proteins (also marked with *asterisks*). The results shown are from two independent experiments

predicted structures are almost identical except for a ten amino acid extension in Kv2.1 (from Leu_{66} to Asp_{76}; Fig. 8b,c) of a docking loop at the lateral part of T1 (in Kv1.4, it is a site of interaction with Kv1β [21]). To test the possibility that the extension of the docking loop mediates the Kv2.1 interaction with VAMP2, we created the Kv2.1$\Delta N_{70\text{-}73}$ mutant (Fig. 9a) by deleting four amino acids at the central part of the extension (Asp_{70} to Ser_{73}; marked with asterisks in Fig. 8c) and tested its ability to interact with VAMP2. The functional interaction of this mutant with VAMP2 was impaired; namely, the shift of $Vi_{1/2}$ by VAMP2 was small and statistically insignificant (Fig. 9b–d). Concomitant reduction by almost fourfold in the binding of VAMP2 was observed (Fig. 9e). These results indicated that the binding of VAMP2 to the N terminus, at or near a site comprising the Kv2.1 extended docking loop, is essential for the effect of VAMP2 on Kv2.1 inactivation.

Kv2.1 protein interacts physically with VAMP2 in rat brain Finally, we aimed to demonstrate the interaction between Kv2.1 and VAMP2 in native tissues using two approaches. First, a "pull-down" assay, using immobilized GST-$N_{1\text{-}184}$ and brain membrane lysates, revealed a prominent VAMP2-immunoreactive band pulled down from the brain membranes by GST-$N_{1\text{-}184}$, as compared with GST itself (Fig. 10a). A reciprocal assay revealed a prominent Kv2.1-immunoreactive band pulled down from the brain membranes by GST-VAMP, as compared with GST itself (Fig. 10b). Second, VAMP2 was co-precipitated with Kv2.1 using an antibody against the C terminus of Kv2.1 (Fig. 10c). To verify the specificity of this interaction, we blocked the co-precipitation by pre-incubation of the antibody with the peptide (+*pep*) against which the antibody was raised and performed a reciprocal experiment where Kv2.1 was co-precipitated with VAMP2 using an antibody against VAMP2.

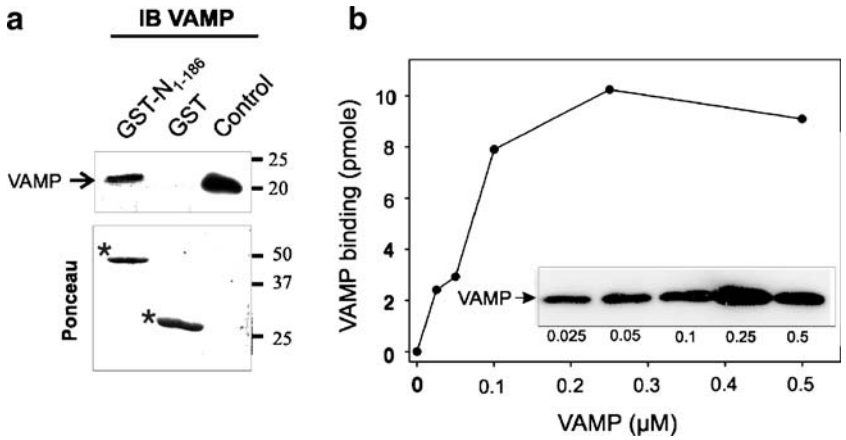

Fig. 6 VAMP2 binds recombinant Kv2.1 N terminus. **a** Purified His6-tagged VAMP2 binds the GST fusion protein corresponding to the N terminus of Kv2.1 (*GST-N_{1-184}*) in vitro. **b** Stoichiometry of the binding of VAMP2 to the N terminus of Kv2.1, derived from binding curves that show saturation. His-6-tagged VAMP2 at the indicated concentrations was bound to immobilized GST-N_{1-184} (20 pmol). Bound VAMP2 was determined by IB with VAMP2 antibody (*inset*), and GST-N_{1-184} was determined by Ponceau staining (data not shown). ECL signal intensities were quantified with TINA software and converted to picomoles by the use of standard curves for the corresponding proteins. *Numbers on the right* refer to the mobility of pre-stained molecular mass standards

Discussion

Plasma membrane VAMP2 interacts physically and functionally with Kv2 channels In this study, strong evidence is presented indicating direct interaction between plasma membrane VAMP2 and Kv2 channels that mediates enhancement of their inactivation. In accord with the proposed role for the N terminus of the channel in the U-shaped inactivation (see "Introduction"), we identified the possible site for VAMP2 interaction in the N terminus near the extended docking loop in the lateral part of the T1 domain of Kv2.1. Given the proposed role for plasma membrane VAMP2 in the regulation of the vesicle cycle [12], the VAMP2 interaction may be important for

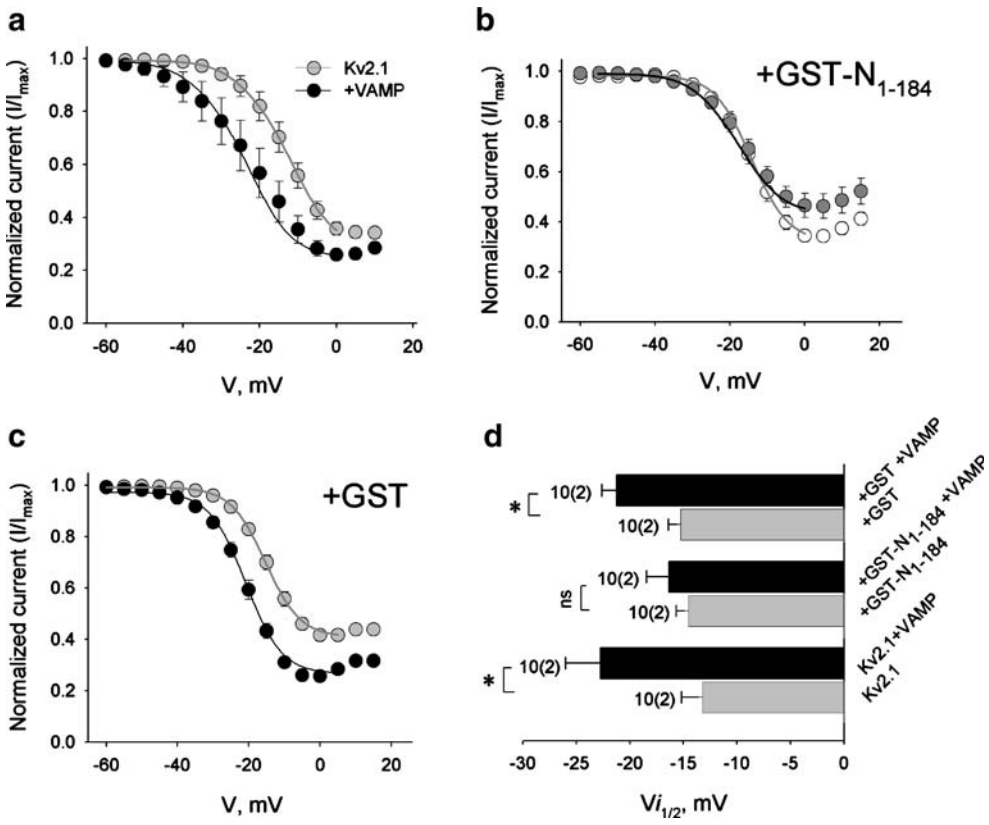

Fig. 7 GST-N_{1-184}, injected 30 to 40 min before the electrophysiological assay of Kv2.1 currents, reverses the effect of co-expressed VAMP2 on Kv2.1 inactivation. *a–c* Representative experiments with oocytes expressing Kv2.1 alone or together with VAMP2 that were either injected before the assay with 3 μM GST-N_{1-184} (**b**) or with GST itself (**c**), or were not injected (**a**). **d** Mean $Vi_{1/2}$ values are shown in $^*p<0.05$

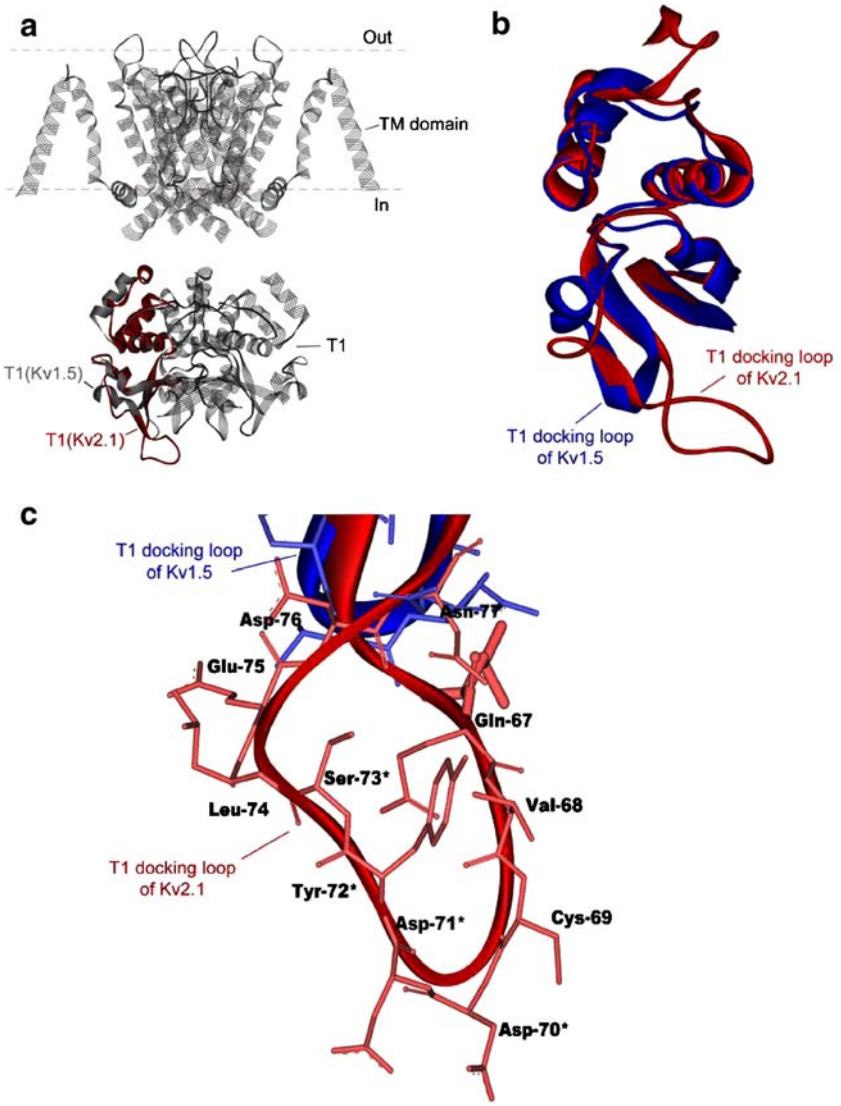

Fig. 8 Identification of "extended docking loop" in the lateral part of Kv2.1 T1 domain. **a** Structural models of Kv2.1 (*red*) and Kv1.5 (*gray*) T1 domains based on the crystal structure of Kv1.2 [40] were fitted with each other and superimposed with the model of Kv1.2 tetramer (depicted in *dimmed gray color*). This view illustrates the relative placement of predicted T1 domains within the channel tetramer. The S1–T1 linkers are omitted; *dashed lines* represent the approximate boundaries of the lipid bilayer. **b** Structure alignment of Kv2.1 (*red*) and Kv1.5 (*blue*) T1 models reveals extension in the docking loop in the lateral part of Kv2.1 N terminus. **c** Predicted Kv2.1 docking loop is about ten amino acids longer than the corresponding structure at the N terminus of Kv1.5. Amino acids deleted in Kv2.1$\Delta N_{70–73}$ are marked with *asterisks*

regulation of release in neuroendocrine cells and neuronal dendrites where DCVs containing hormones, neuropeptides, or neurotrophins and Kv2.1 channels are co-localized. This interaction, occurring at the N terminus, could possibly occur concomitantly with the interaction of Syx at the C terminus; the latter interaction has been recently shown to enhance the release of DCVs [54, 55]. Thus, alongside with the Syx interaction [55], the VAMP2 interaction may contribute to the activity dependence of DCV release (see below).

Effect of VAMP2 on Kv2 inactivation Kv2 channels undergo slow U-shaped inactivation from preferentially partially activated closed states [31]. We found that VAMP2 regulates the steady-state and kinetic parameters of both Kv2.1 and Kv2.2 inactivation. The channels inactivate at more hyperpolarizing potentials with accelerated inactivation onset and slowed down recovery from inactivation. In all, interaction with VAMP2 renders the inactivation state more favorable, downregulating the potassium current, which could serve an important physiological purpose (see below).

Kv2.1 N terminus mediates the effect of VAMP2 on the U-type inactivation: a possible mechanism The tetramerization (T1) domain of K^+ channels has been found to adopt BTB/POZ folding motif. This conserved protein–protein interaction motif, observed in various protein complexes, provides multiple binding faces for other proteins found within this fold [2]. Proteins with BTB/POZ organization usually mediate homomeric and, in some instances, heteromeric dimerization and also serve as receptors for different regulatory proteins. It was already demonstrated that T1 domains of Kv channels can interact with the GTPase protein RhoA [7], a tyrosine phosphatase [57], Kvβs [21], and a variety of accessory subunits, including KChIPs and

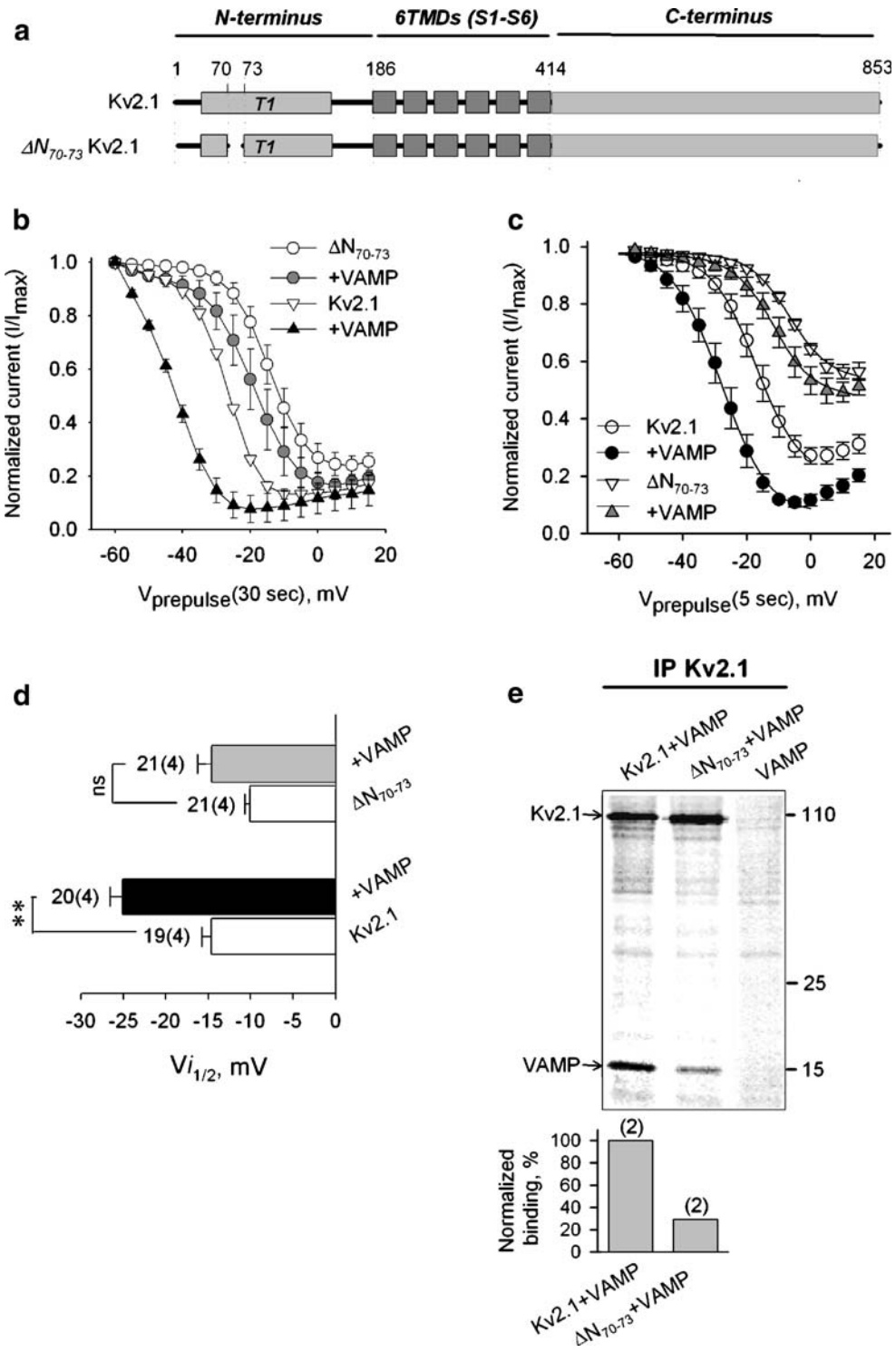

Fig. 9 Partial deletion of the Kv2.1 "extended docking loop" abolished the effect of VAMP2 on Kv2.1 inactivation. **a** Schematic presentation of N-terminal deletion mutants. Representative experiments with 30-s (**b**) and 5-s (**c**) inactivation protocols, demonstrating the effect of VAMP2 on Kv2.1ΔN_{70-73} inactivation. **d** Mean $Vi_{1/2}$ values obtained from four independent experiments using 5-s inactivation protocol; *numbers without parentheses* denote the total number of oocytes per group. **e** Digitized Phosphorimager scan of SDS-PAGE analysis of the [^{35}S]Met/Cys-labeled mutants injected with VAMP2 and immunoprecipitated by an antibody raised against the C terminus of Kv2.1 (*IP Kv2.1*). The *bar diagram* below the scan demonstrate normalized VAMP2 to channel binding. $^{**}p<0.001$; *ns* difference is statistically not significant

KChAPs (reviewed in [49]). In spite of the fact that four T1 domains are attached to the corresponding gate-forming transmembrane segments as a structurally separated cytoplasmic "hanging gondola" [32], it has been demonstrated in a number of studies that structural and conformational changes in the T1 domain can dramatically affect Kv channels activation and inactivation gating. As for inactivation gating, it was demonstrated that the Kv2.1 T1 domain is important for the U-shaped inactivation, and when transferred to Kv1.5, it conveys U-shaped inactivation to Kv1.5 [35]. Relevant to our study, two regulatory proteins, Kvβs and KChIPs, were shown to affect the inactivation gating of various target voltage-gated K^+ channels by binding to distinct sites via docking loops at

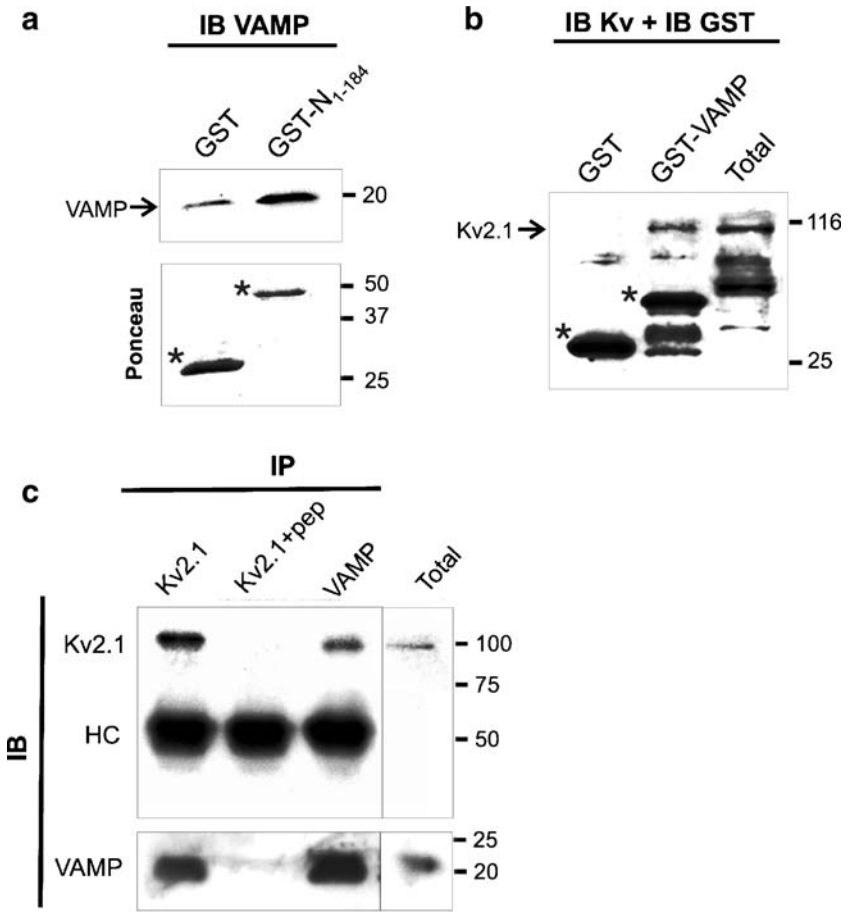

Fig. 10 Kv2.1 protein could associate with VAMP2 in native tissues. GST-N_{1-184} (**a**) and GST-VAMP2 (**b**) fusion proteins pull down VAMP2 and Kv2.1, correspondingly, from rat brain membranes. Proteins were immunoblotted (*IB*) with either anti-VAMP antibody (*IB VAMP*) or anti-Kv2.1/anti-GST antibodies (*IB Kv2.1 + IB GST*). **c** Kv2.1 interacts with VAMP2 in rat brain membranes. Proteins were immunoprecipitated (*IP*) by Kv2.1 (in the absence and presence of antigen peptide (+*pep*; 1:1 ratio) or VAMP2 antibodies, as indicated *above the lanes*. The precipitated proteins were separated by SDS-PAGE, blotted, and detected by antibodies (IB), as indicated on the *left* side of the blot; *HC* heavy chain of the antibodies used. For each IP reaction, we used 200 mg of lysate; 1 mg of lysate was loaded on *Total* lane (no immunoprecipitation was performed). Molecular weight markers are shown on the *right*. *Arrows* indicate the migration of the denoted proteins (also marked with *asterisks* on the gel scan)

the lateral parts of their T1: Kvβs interact with Kv1.x (reviewed in [42]), Kv4.x [46], and Kv2.2 [18], and KChIPs interact with Kv4.x [1, 9]. Although the action of both regulatory proteins involves N-terminal association, their mechanisms to regulate inactivation are different. In the case of Kvβ, one monomer binds one T1 domain right from below the gondola [21] and confers rapid inactivation by its N terminus, inactivating ball [50] that accesses the pore through entering a lateral opening between the T1 and the membrane-spanning domains [21]. In the case of KChiP, one molecule binds two neighboring T1 domains [61], clamping their N termini, resulting in substantial slowing of inactivation and acceleration of recovery from inactivation [4, 22]. The mechanism of KChIPs to regulate inactivation most likely involves interference with voltage-dependent gating rearrangements in the intracellular T1–T1 interface of a K^+ channel [9, 60], which are coupled, either allosterically or directly, to conformational changes in the gate-forming transmembrane domains. As KChIP clamps T1 domains, it also obstructs the movement of the gate-forming transmembrane domain and therefore could stabilize either the open or the closed state of the channel [63].

That VAMP2 enhances Kv2.1 U-type inactivation via interaction with T1 domains and that inter-subunit T1 domain interactions were shown to influence Kv2.1 U-type inactivation [35] may provide a potential mechanism, somewhat similar to the mode of action of KChIP for the interaction of VAMP2 with Kv2.1. In such a scenario, while the C terminus of VAMP is anchored into the plasma membrane, the N-terminal or SNARE domains of VAMP2 may bind near or at the docking loop, rendering the T1 domain less mobile and consequently interfering with

voltage-dependent T1–T1 rearrangements to impair full opening of the channels which inactivate from partially activated closed state.

Physiological relevance of the interaction between VAMP2 and Kv2.1 Significant amount of VAMP has been observed in the plasma membrane in various neuronal cells. The main source of this VAMP pool is fusion of vesicles with the plasma membrane [12]. This surface VAMP pool is determined by the rates of exocytosis and endocytosis and consequently correlates with recent synaptic activity [12].

Recently, it was demonstrated that the sustained current carried by Kv2.1 plays a major role during high-frequency stimulation in regulating spike duration and consequent regulation of calcium entry in dendrites of CA1 pyramidal neurons [13]. Given the activity dependence of VAMP2 surface abundance [11], upon intense activity, VAMP2 can associate with Kv2.1 channels to trim down the sustained K^+ currents, leading to membrane depolarization and subsequent rise in intracellular Ca^{2+} concentration. This rise in intracellular Ca^{2+} could work as positive feedback, contributing to Ca^{2+}-dependent refilling of the readily releasable pool of synaptic vesicles and, alongside with the established effect of VAMP2 to recycle exocytosed vesicles by fast endocytosis [11], could contribute to the activity dependence of DCV release from dendrites.

Acknowledgments We thank Prof. David Fedida for the Kv1.5N/Kv2.1 construct, Dr. Michael Veit for His-6-tagged VAMP-2 construct, and Prof. José López-Barneo for the Kv2.1/Kv2.3NRD construct. This work was supported by grants from the Israel Science Foundation (I.L.).

References

1. An WF, Bowlby MR, Betty M, Cao J, Ling HP, Mendoza G, Hinson JW, Mattsson KI, Strassle BW, Trimmer JS, Rhodes KJ (2000) Modulation of A-type potassium channels by a family of calcium sensors. Nature 403:553–556
2. Bardwell VJ, Treisman R (1994) The POZ domain: a conserved protein–protein interaction motif. Genes Dev 8:1664–1677
3. Bates PA, Kelley LA, MacCallum RM, Sternberg MJ (2001) Enhancement of protein modeling by human intervention in applying the automatic programs 3D-JIGSAW and 3D-PSSM. Proteins Suppl 5:39–46
4. Beck EJ, Bowlby M, An WF, Rhodes KJ, Covarrubias M (2002) Remodelling inactivation gating of Kv4 channels by KChIP1, a small-molecular-weight calcium-binding protein. J Physiol 538:691–706
5. Bennett MK (1995) SNAREs and the specificity of transport vesicle targeting. Curr Opin Cell Biol 7:581–586
6. Braun JE, Fritz BA, Wong SM, Lowe AW (1994) Identification of a vesicle-associated membrane protein (VAMP)-like membrane protein in zymogen granules of the rat exocrine pancreas. J Biol Chem 269:5328–5335
7. Cachero TG, Morielli AD, Peralta EG (1998) The small GTP-binding protein RhoA regulates a delayed rectifier potassium channel. Cell 93:1077–1085
8. Calakos N, Bennett MK, Peterson KE, Scheller RH (1994) Protein–protein interactions contributing to the specificity of intracellular vesicular trafficking. Science 263:1146–1149
9. Callsen B, Isbrandt D, Sauter K, Hartmann LS, Pongs O, Bahring R (2005) Contribution of N- and C-terminal Kv4.2 channel domains to KChIP interaction [corrected]. J Physiol 568:397–412
10. Chiara MD, Monje F, Castellano A, Lopez-Barneo J (1999) A small domain in the N terminus of the regulatory alpha-subunit Kv2. 3 modulates Kv2.1 potassium channel gating. J Neurosci 19:6865–6873
11. Deák F, Schoch S, Liu X, Südhof TC, Kavalali ET (2004) Synaptobrevin is essential for fast synaptic-vesicle endocytosis. Nat Cell Biol 6:1102–1108
12. Dittman JS, Kaplan JM (2006) Factors regulating the abundance and localization of synaptobrevin in the plasma membrane. Proc Natl Acad Sci USA 103:11399–11404
13. Du J, Haak LL, Phillips-Tansey E, Russell JT, McBain CJ (2000) Frequency-dependent regulation of rat hippocampal somato-dendritic excitability by the K^+ channel subunit Kv2.1. J Physiol 522(Pt 1):19–31
14. Du J, Tao-Cheng JH, Zerfas P, McBain CJ (1998) The K^+ channel, Kv2.1, is apposed to astrocytic processes and is associated with inhibitory postsynaptic membranes in hippocampal and cortical principal neurons and inhibitory interneurons. Neuroscience 84:37–48
15. Evans RM, Zamponi GW (2006) Presynaptic Ca^{2+} channels—integration centers for neuronal signaling pathways. Trends Neurosci 29:617–624
16. Fernandez-Alfonso T, Kwan R, Ryan TA (2006) Synaptic vesicles interchange their membrane proteins with a large surface reservoir during recycling. Neuron 51:179–186
17. Fili O, Michaelevski I, Bledi Y, Chikvashvili D, Singer-Lahat D, Boshwitz H, Linial M, Lotan I (2001) Direct interaction of a brain voltage-gated K^+ channel with syntaxin 1A: functional impact on channel gating. J Neurosci 21:1964–1974
18. Fink M, Duprat F, Lesage F, Heurteaux C, Romey G, Barhanin J, Lazdunski M (1996) A new K^+ channel beta subunit to specifically enhance Kv2.2 (CDRK) expression. J Biol Chem 271:26341–26348
19. Foster LJ, Weir ML, Lim DY, Liu Z, Trimble WS, Klip A (2000) A functional role for VAP-33 in insulin-stimulated GLUT4 traffic. Traffic 1:512–521
20. Frech GC, VanDongen AM, Schuster G, Brown AM, Joho RH (1989) A novel potassium channel with delayed rectifier properties isolated from rat brain by expression cloning. Nature 340:642–645
21. Gulbis JM, Zhou M, Mann S, MacKinnon R (2000) Structure of the cytoplasmic beta subunit-T1 assembly of voltage-dependent K^+ channels. Science 289:123–127
22. Holmqvist MH, Cao J, Hernandez-Pineda R, Jacobson MD, Carroll KI, Sung MA, Betty M, Ge P, Gilbride KJ, Brown ME, Jurman ME, Lawson D, Silos-Santiago I, Xie Y, Covarrubias M, Rhodes KJ, Distefano PS, An WF (2002) Elimination of fast inactivation in Kv4 A-type potassium channels by an auxiliary subunit domain. Proc Natl Acad Sci USA 99:1035–1040
23. Hwang PM, Fotuhi M, Bredt DS, Cunningham AM, Snyder SH (1993) Contrasting immunohistochemical localizations in rat brain of two novel K^+ channels of the Shab subfamily. J Neurosci 13:1569–1576
24. Hwang PM, Glatt CE, Bredt DS, Yellen G, Snyder SH (1992) A novel K^+ channel with unique localizations in mammalian brain: molecular cloning and characterization. Neuron 8:473–481

25. Ivanina T, Perets T, Thornhill WB, Levin G, Dascal N, Lotan I (1994) Phosphorylation by protein kinase A of RCK1 K^+ channels expressed in *Xenopus oocytes*. Biochemistry 33:8786–8792
26. Ji J, Tsuk S, Salapatek AM, Huang X, Chikvashvili D, Pasyk EA, Kang Y, Sheu L, Tsushima R, Diamant N, Trimble WS, Lotan I, Gaisano HY (2002) The 25-kDa synaptosome-associated protein (SNAP-25) binds and inhibits delayed rectifier potassium channels in secretory cells. J Biol Chem 277:20195–20204
27. Kammer B, Schmidt MF, Veit M (2003) Functional characterization of palmitoylated and nonacylated SNAP-25 purified from insect cells infected with recombinant baculovirus. Mol Cell Neurosci 23:333–340
28. Kerschensteiner D, Monje F, Stocker M (2003) Structural determinants of the regulation of the voltage-gated potassium channel Kv2.1 by the modulatory alpha-subunit Kv9.3. J Biol Chem 278:18154–18161
29. Kerschensteiner D, Stocker M (1999) Heteromeric assembly of Kv2.1 with Kv9.3: effect on the state dependence of inactivation. Biophys J 77:248–257
30. Klemic KG, Kirsch GE, Jones SW (2001) U-type inactivation of Kv3.1 and Shaker potassium channels. Biophys J 81:814–826
31. Klemic KG, Shieh CC, Kirsch GE, Jones SW (1998) Inactivation of Kv2.1 potassium channels. Biophys J 74:1779–1789
32. Kobertz WR, Williams C, Miller C (2000) Hanging gondola structure of the T1 domain in a voltage-gated K(+) channel. Biochemistry 39:10347–10352
33. Kurata HT, Doerksen KW, Eldstrom JR, Rezazadeh S, Fedida D (2005) Separation of P/C- and U-type inactivation pathways in Kv1.5 potassium channels. J Physiol 568:31–46
34. Kurata HT, Fedida D (2006) A structural interpretation of voltage-gated potassium channel inactivation. Prog Biophys Mol Biol 92:185–208
35. Kurata HT, Soon GS, Eldstrom JR, Lu GW, Steele DF, Fedida D (2002) Amino-terminal determinants of U-type inactivation of voltage-gated K^+ channels. J Biol Chem 277:29045–29053
36. Leung YM, Kang Y, Gao X, Xia F, Xie H, Sheu L, Tsuk S, Lotan I, Tsushima RG, Gaisano HY (2003) Syntaxin 1A binds to the cytoplasmic C terminus of Kv2.1 to regulate channel gating and trafficking. J Biol Chem 278:17532–17538
37. Levin G, Chikvashvili D, Singer-Lahat D, Peretz T, Thornhill WB, Lotan I (1996) Phosphorylation of a K^+ channel alpha subunit modulates the inactivation conferred by a beta subunit. Involvement of cytoskeleton. J Biol Chem 271:29321–29328
38. Levin G, Keren T, Peretz T, Chikvashvili D, Thornhill WB, Lotan I (1995) Regulation of RCK1 currents with a cAMP analog via enhanced protein synthesis and direct channel phosphorylation. J Biol Chem 270:14611–14618
39. Linial M, Ilouz N, Parnas H (1997) Voltage-dependent interaction between the muscarinic ACh receptor and proteins of the exocytic machinery. J Physiol 504(Pt 2):251–258
40. Long SB, Campbell EB, Mackinnon R (2005) Crystal structure of a mammalian voltage-dependent Shaker family K^+ channel. Science 309:897–903
41. MacDonald PE, Wang G, Tsuk S, Dodo C, Kang Y, Tang L, Wheeler MB, Cattral MS, Lakey JR, Salapatek AM, Lotan I, Gaisano HY (2002) Synaptosome-associated protein of 25 kilodaltons modulates Kv2.1 voltage-dependent K(+) channels in neuroendocrine islet beta-cells through an interaction with the channel N terminus. Mol Endocrinol 16:2452–2461
42. Martens JR, Kwak YG, Tamkun MM (1999) Modulation of Kv channel alpha/beta subunit interactions. Trends Cardiovasc Med 9:253–258
43. Michaelevski I, Chikvashvili D, Tsuk S, Fili O, Lohse MJ, Singer-Lahat D, Lotan I (2002) Modulation of a brain voltage-gated K^+ channel by syntaxin 1A requires the physical interaction of Gbetagamma with the channel. J Biol Chem 277:34909–34917
44. Michaelevski I, Chikvashvili D, Tsuk S, Singer-Lahat D, Kang Y, Linial M, Gaisano HY, Fili O, Lotan I (2003) Direct interaction of target SNAREs with the Kv2.1 channel. Modal regulation of channel activation and inactivation gating. J Biol Chem 278:34320–34330
45. Murakoshi H, Trimmer JS (1999) Identification of the Kv2.1 K^+ channel as a major component of the delayed rectifier K^+ current in rat hippocampal neurons. J Neurosci 19:1728–1735
46. Nakahira K, Shi G, Rhodes KJ, Trimmer JS (1996) Selective interaction of voltage-gated K^+ channel beta-subunits with alpha-subunits. J Biol Chem 271:7084–7089
47. Nevins AK, Thurmond DC (2005) A direct interaction between Cdc42 and vesicle-associated membrane protein 2 regulates SNARE-dependent insulin exocytosis. J Biol Chem 280:1944–1952
48. Pennuto M, Bonanomi D, Benfenati F, Valtorta F (2003) Synaptophysin I controls the targeting of VAMP2/synaptobrevin II to synaptic vesicles. Mol Biol Cell 14:4909–4919
49. Pourrier M, Schram G, Nattel S (2003) Properties, expression and potential roles of cardiac K^+ channel accessory subunits: MinK, MiRPs, KChIP, and KChAP. J Membr Biol 194:141–152
50. Rettig J, Heinemann SH, Wunder F, Lorra C, Parcej DN, Dolly JO, Pongs O (1994) Inactivation properties of voltage-gated K^+ channels altered by presence of beta-subunit. Nature 369:289–294
51. Roe MW, Worley JF 3rd, Mittal AA, Kuznetsov A, DasGupta S, Mertz RJ, Witherspoon SM 3rd, Blair N, Lancaster ME, McIntyre MS, Shehee WR, Dukes ID, Philipson LH (1996) Expression and function of pancreatic beta-cell delayed rectifier K^+ channels. Role in stimulus-secretion coupling. J Biol Chem 271:32241–32246
52. Schiavo G, Benfenati F, Poulain B, Rossetto O, Polverino de Laureto P, DasGupta BR, Montecucco C (1992) Tetanus and botulinum-B neurotoxins block neurotransmitter release by proteolytic cleavage of synaptobrevin. Nature 359:832–835
53. Sherry DM, Wang MM, Frishman LJ (2003) Differential distribution of vesicle associated membrane protein isoforms in the mouse retina. Mol Vis 9:673–688
54. Singer-Lahat D, Chikvashvili D, Lotan I (2008) Direct interaction of endogenous Kv channels with Syntaxin enhances exocytosis by neuroendocrine cells. PLoS ONE 3:e1381
55. Singer-Lahat D, Sheinin A, Chikvashvili D, Tsuk S, Greitzer D, Friedrich R, Feinshreiber L, Ashery U, Benveniste M, Levitan ES, Lotan I (2007) K^+ channel facilitation of exocytosis by dynamic interaction with syntaxin. J Neurosci 27:1651–1658
56. Taubenblatt P, Dedieu JC, Gulik-Krzywicki T, Morel N (1999) VAMP (synaptobrevin) is present in the plasma membrane of nerve terminals. J Cell Sci 112(Pt 20):3559–3567
57. Tsai W, Morielli AD, Cachero TG, Peralta EG (1999) Receptor protein tyrosine phosphatase alpha participates in the m1 muscarinic acetylcholine receptor-dependent regulation of Kv1.2 channel activity. The EMBO J 18:109–118
58. Tsuk S, Michaelevski I, Bentley GN, Joho RH, Chikvashvili D, Lotan I (2005) Kv2.1 channel activation and inactivation is influenced by physical interactions of both syntaxin 1A and the syntaxin 1A/soluble *N*-ethylmaleimide-sensitive factor-25 (t-SNARE) complex with the C terminus of the channel. Mol Pharmacol 67:480–488
59. VanDongen AM, Frech GC, Drewe JA, Joho RH, Brown AM (1990) Alteration and restoration of K^+ channel function by deletions at the N- and C-termini. Neuron 5:433–443
60. Wang G, Covarrubias M (2006) Voltage-dependent gating rearrangements in the intracellular T1-T1 interface of a K^+ channel. J Gen Physiol 127:391–400

61. Wang H, Yan Y, Liu Q, Huang Y, Shen Y, Chen L, Chen Y, Yang Q, Hao Q, Wang K, Chai J (2007) Structural basis for modulation of Kv4 K^+ channels by auxiliary KChIP subunits. Nat Neurosci 10:32–39
62. Wolf-Goldberg T, Michaelevski I, Tsuk S, Chikvashvili D, Lotan I (2006) Regulation by t-SNAREs of Kv2.2 activation and inactivation gating is different from that of Kv2.1: implications to underlying protein–protein interactions
63. Yi BA, Minor DL Jr., Lin YF, Jan YN, Jan LY (2001) Controlling potassium channel activities: interplay between the membrane and intracellular factors. Proc Natl Acad Sci USA 98:11016–11023